The Structure of the Bacteriophage T4 Cell-puncturing Device

P. G. Leiman,[1] S. Kanamaru,[1] V. A. Kostyuchenko,[2] P.R. Chipman,[1]
V. V. Mesyanzhinov,[2] F. Arisaka,[3] M. G. Rossmann[1]
[1]Purdue University, West Lafayette, IN, U.S.A.
[2]Shemyakin-Ovchinnikov Institute of Bioorganic Chemistry, Moscow, Russia
[3]Tokyo Institute of Technology, Yokohama, Japan

Introduction

Bacteriophage T4 has a very efficient mechanism for infecting cells [1]. The key component of the infection process is the baseplate, located at the end of the phage tail, which regulates the interaction of the tail fibers and the DNA ejection machine [2]. The complex of gene product 5 (gp5) (63 kDa) and gp27 (44 kDa), the central part of the baseplate, is required to penetrate the *E. coli* outer cell membrane and to disrupt the intermembrane peptidoglycan layer, promoting subsequent phage DNA entry into the host. We set our goal to determine the crystal structure of the gp5-gp27 complex to elucidate the initial steps of the infection process.

The center of the baseplate, or hub, consists of at least two phage proteins, gp5 and gp27 [3, 4], which form a stable complex *in vivo* and *in vitro*. Phage mutants lacking either of these proteins produce hubless baseplates and, as a result, are tailless and noninfectious. The hub has lysozyme activity attributed to the lysozyme domain of gp5, which is required to digest the cellular intermembrane peptidoglycan layer during phage tail contraction [5]. The gp5 lysozyme domain has 43% sequence identity [6] with the cytoplasmic T4 lysozyme (T4L) [7]. Unlike T4L, gp5 lysozyme activity is essential for phage growth and infection [8]. When incorporated into the phage baseplate or stored at high concentration, gp5 undergoes maturational cleavage between Ser351 and Ala352, but both resultant parts — the N-terminal part (gp5*) and the C-terminal part (gp5C) (Fig. 1a) — remain in the phage particle [9]. Gp5C is an SDS-resistant trimer, rich in β structure [9], containing 11 **V**X**G**XXXXX sequence repeats [6, 9] (Fig. 1b). The complex of gp5 with gp27 obtained *in vivo* and *in vitro* contains both gp5* and gp5C, thus constituting a heterononameric assembly $(gp27\text{-}gp5^*\text{-}gp5C)_3$ (Fig. 1c). At elevated temperatures, this complex dissociates into three (gp27-gp5*) heterodimers and a $(gp5C)_3$ homotrimer, showing that gp5C is necessary for trimerization of the entire complex [9] (Fig. 1c). However, dissociation of gp5* from gp27 can occur only at low pH (S. Kanamaru, Y. Takeda, and F. Arisaka, in preparation). The lysozyme activity of the trimeric gp5*, when stabilized by gp5C, is an order of magnitude less than the activity of the monomeric gp5* [9].

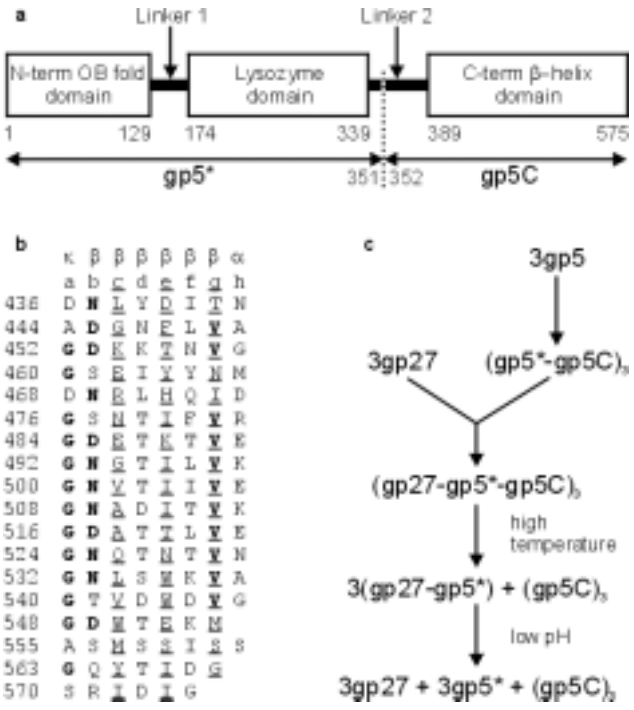

FIG. 1. Assembly of $(gp27\text{-}gp5^*\text{-}gp5C)_3$.
a = Domain organization within the gp5 monomer. The maturation cleavage is indicated by the dotted line. Initial and final residue numbers are shown for each domain.
b = Alignment of the octapeptide units composing the intertwined part of the carboxy-terminal β-helix domain of gp5. Conserved residues are in bold print; residues facing the inside are underlined. The main chain dihedral angle configuration of each residue in the octapeptide is indicated at the top by κ (kink), β (sheet), and α (helix).
c = Assembly of gp5 and gp27 into the hub and needle of the baseplate.

Methods and Materials

Separate expression vectors containing gene 5 and gene 27 and a coexpression vector were constructed (S. Kanamaru, Y. Takeda, and F. Arisaka, in preparation). The gp5-gp27 complex was purified with the aid of a gp5 C-terminal His tag. Crystals were formed in hanging

drops at 12°C from 5.2% PEG 8000, 0.65 M Tris pH 8.5, and 35% glycerol. They belonged to space group *R*32, with cell dimensions of $a = 138.1$ and $c = 388.9$ Å. SeMet-substituted gp5 was insoluble, but, fortunately, the SeMet-substituted gp27 was soluble. A chimerical complex containing separately expressed native gp5 and the SeMet-substituted gp27 was purified and crystallized. Four-wavelength multiple anomalous dispersion data were collected by using the chimerical crystals of the complex that diffracted to 2.9-Å resolution. Fifteen of the total of 16 Se in the gp27 monomer were found with the help of the program SHELX [10]. These sites were refined and used to obtain phases with the program MLPHARE [11]. The phases were then improved by solvent flipping by using the program CNS [12]. The resultant electron density map was easily interpreted by using the graphics program XtalView [13]. Refinement of the atomic model with the program CNS [19] converged to the working *R*-factor of 21% and R_{free} of 28%.

Mutant T4 phage lacking the ability to assemble the tail sheath and head were used to produce the baseplate-tail tube assembly. The 3-D image reconstructions of the baseplate-tail tube assembly were computed by using SPIDER [14]. The baseplate was assumed to be sixfold symmetric. A total of 418 images were employed to obtain a map at about 17-Å resolution.

Results

The crystal structure of the $(gp5\text{-}gp27)_3$ 321 kDa complex has been determined to 2.9-Å resolution fitted into a 17-Å resolution cryo-electron microscopy (cryoEM) image reconstruction of the baseplate-tail tube assembly. The C-terminal domain of gp5 is a 110-Å-long, 28-Å-wide, triple-stranded β-helix, forming an equilateral triangular prism, that acts as a membrane-puncturing needle. The middle lysozyme domain of gp5, situated on the periphery of the prism, serves to digest the peptidoglycan layer. The amino-terminal, antiparallel β–barrel domain of gp5 is inserted into a cylinder formed by three gp27 monomers that may serve as a channel for DNA ejection.

The structure of the $(gp27\text{-}gp5^*\text{-}gp5C)_3$ complex (Fig. 2) resembles a 190-Å-long torch in which the gp27 trimer forms its cylindrical "head" and the gp5C trimer forms the "handle." The gp27 trimer makes a hollow cylinder about 60-Å long, with internal and external diameters of about 30 and 80 Å, respectively, encompassing the three N-terminal domains of gp5* to which the trimeric gp5C torch handle is attached. The carboxy-terminal parts of the three gp5C polypeptide chains fold into a β-helical prism in which the faces have a slight left-handed twist. The middle lysozyme domains surround the amino end of the prism.

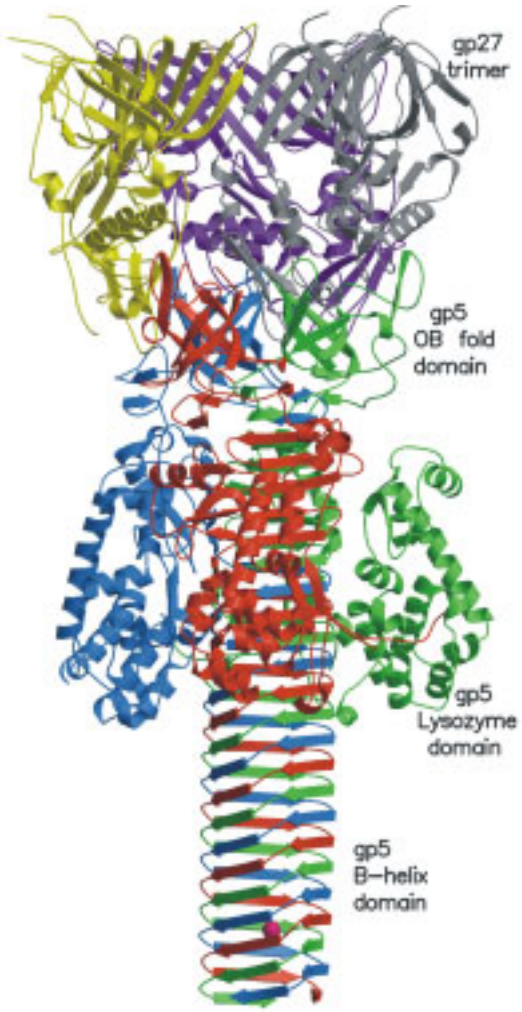

FIG. 2. Ribbon diagram of the $(gp27\text{-}gp5^*\text{-}gp5C)_3$ complex.

Generally, good agreement was observed upon fitting the $(gp27\text{-}gp5^*\text{-}gp5C)_3$ structure into the 17-Å resolution, cryoEM, 3-D image reconstruction of the baseplate-tail tube assembly. As expected, it forms the central hub of the baseplate, with the β-helical prism domain forming a needle pointing toward the potential host surface (Fig. 3). The threefold symmetry of the $(gp27\text{-}gp5^*\text{-}gp5C)_3$ complex contrasts with the assumed sixfold symmetry of the baseplate and may, in part, account for the absence of density representing the lysozyme domain. However, it is also probable that the lysozyme is somewhat disordered in its position, made possible by the long, flexible, linker regions 1 and 2 (Fig. 1a).

Discussion

The $(gp27\text{-}gp5^*\text{-}gp5C)_3$ complex can be fitted into the cryoEM image reconstruction of the T4 baseplate-tail

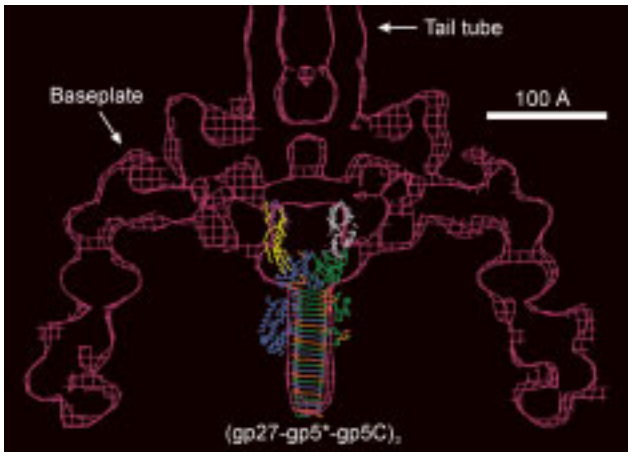

FIG. 3. Cross-sectioned density of the cryoEM reconstruction of the T4 baseplate-tail tube assembly fitted with the atomic (gp27-gp5-gp5C)$_3$ complex structure.*

tube assembly (Fig. 3). The gp27 cylinder is seen to be an extension of the tail tube, which is continued by the three N-terminal domains of gp5. The latter associates with the N end of the β-helix that terminates the extended tube. The three lysozyme domains are located around the β–helix under the baseplate but vary in their exact positions, which could explain the lack of density in the cryoEM reconstruction. The diameter of the gp27 cylinder is of a size that can accommodate a dsDNA helix, thus forming a channel that would allow the DNA to penetrate the tail tube as far as the N-terminal domain of gp5.

Upon attachment of the baseplate to the cell surface, the tail sheath contracts, exerting a force onto the tail tube toward the cell membrane. This force would then be transmitted through the gp27 cylinder and the N-terminal domain of gp5 to the β-helix, causing the latter to puncture the outer membrane. As the tail sheath contraction progresses, the β-helix would be able to span the entire 40-Å width of the outer membrane, thereby enlarging the pore in the membrane. Subsequently, the three lysozyme domains will reach the peptidoglycan layer to digest the cell wall, allowing penetration of the tail tube to the inner membrane for injection of the phage DNA into the host.

Acknowledgments

Use of the APS was supported by the U.S. Department of Energy, Office of Science, Office of Basic Energy Sciences, under Contract No. W-31-109-ENG-38. We thank the staff of the Bio Consortium for Advanced Radiation Sources (BioCARS) for help and advice in data collection. All ribbon diagrams were drawn with MOLSCRIPT [15] and Raster3D [16].

References

The content of this report is based on the following paper: A. Kanamaru, P. G. Leiman, V. A. Kostyuchenko, P. R. Chipman, V. V. Mesyanzhinov, F. Arisaka, and M. G. Rossmann, “Structure of the cell-puncturing device of bacteriophage T4,” Nature **415**, 553-557 (2002).

[1] E. Goldberg, L. Grinius, and L. Letellier, in *Molecular Biology of Bacteriophage T4*, edited by J. D. Karam (American Society for Microbiology, Washington, DC, 1994), p. 347-356.

[2] D. H. Coombs and F. Arisaka, in *Molecular Biology of Bacteriophage T4*, edited by J. D. Karam (American Society for Microbiology, Washington, DC, 1994), p. 259-281.

[3] Y. Kikuchi and J. King, J. Mol. Biol. **99**, 695-716 (1975).

[4] R. W Vanderslice and C. D Yegian, Virol. **60**, 265-275 (1974).

[5] H. Nakagawa, F. Arisaka, and S. Ishii, J. Virol. **54**, 460-466 (1985).

[6] G. Mosig, G. W. Lin, J. Franklin, and W. H. Fan, New Biol. **1**, 171-179 (1989).

[7] B. W. Matthews and S. J. Remington, Proc. Natl. Acad. Sci. U.S.A. **71**, 4178-4182 (1974).

[8] S. Takeda, K. Hoshida, and F. Arisaka, Biochim. Biophys. Acta **1384**, 243-252 (1998).

[9] S. Kanamaru, N. C. Gassner, N. Ye, S. Takeda, and F. Arisaka, J. Bacteriol. **181**, 2739-2744 (1999).

[10] G. M. Sheldrick, in *International Tables for Crystallography Vol. F: Crystallography of Biological Macromolecules*, edited by M. G. Rossmann and E. Arnold (Kluwer Academic Publishers, Dordrecht/Boston/London, 2001), pp. 734-738.

[11] Z. Otwinowski, in *Proceedings of the CCP4 Study Weekend, 25-26 January 1991*, edited by W. Wolf, P. R. Evans, and A. G. W. Leslie (Science and Engineering Research Council, Daresbury, England, 1991), p. 80-86.

[12] A. T. Brünger et al,. Acta Crystallogr. D **54**, 905-921 (1998).

[13] D. E. McRee, J. Struct. Biol. **125**, 156-165 (1999).

[14] J. Frank et al., J. Struct. Biol. **116**, 190-199 (1996).

[15] P. Kraulis, J. Appl. Crystallogr. **24**, 946-950 (1991).

[16] E. A. Merritt and D. J. Bacon, Meth. Enzymol. **277**, 505-524 (1997).